to FAD is demonstrated by the ability to detect FAD from solutions as low as 10^{-10} M. When the amount of free flavin in the GO preparation is reduced by purification (as evidenced by low relative fluorescence of the adsorbing solution), the SERRS spectrum of GO is severely attenuated or nonexistent under our experimental conditions. Additionally, a correlation is observed to exist between the corrected relative fluorescence of the adsorbing solution and the intensity of the resulting flavin SERRS spectrum. This indicates that the SERRS active species adsorbed onto the electrode is actually free flavin. The free flavin is not produced by the adsorption of GO onto the electrode but is released spontaneously from the protein in solution. On the other hand, FAD is released from the enzyme if the electrode anodization is performed in the presence of the enzyme. Because of the extreme sensitivity of SERRS to FAD, consideration of its potential interference should be made in future SERRS investigations of GO or other flavoproteins.

The relevance of these results to SERRS studies of flavoproteins and proteins in general is clear. First, it is essential that highly purified protein preparations be employed. It is apparent that a chemical enhancement mechanism is involved in the SERRS spectrum of FAD and this obscures any long-range enhancement that might be present. The chromophore in the native enzyme is apparently not able to interact directly with the silver, either due to the presence of the protein envelope or because the orientation of the adsorbed protein prevents this. The presence of impurities (especially those which are resonantly enhanced) which adsorbed strongly onto Ag may result in spectra which are artifactual. Second, the adsorption of large biological molecules onto metal electordes does not necessarily produce denaturation or the loss of noncovalently bound cofactors. However, anodization of the electrode in the presence of the adsorbate can produce these effects. Third, SERRS may provide a means for detecting partially denatured protein or free chromophore in other proteins as well. It has already been shown that SERS can be utilized to detect low concentrations of denatured DNA.[22]

Acknowledgment. The authors gratefully acknowledge the National Institutes of Health for support of this work in the form of Grant GM 35108-03. We thank Professor Fred Wagner for discussions regarding the preparation and purification of glucose oxidase. We are also grateful to Professor Tom Spiro and Dr. Robert Copeland for helpful discussions and to Professor Michael Morris for providing us with preprints of his FAD and flavoprotein results.

Registry No. FAD, 146-14-5; GO, 9001-37-0.

(22) (a) Koglin, E.; Sèquaris, J.-M. *Top. Current Chem.* **1986**, *134*, 1-57 and references cited therein. (b) Brabec, V.; Niki, K. *Biophys. Chem.* **1985**, *23*, 63-70.

Theoretical Study of the Ground- and Excited-State Reactivity of Na + FH. Comparison of SCF-CI and VB Treatments

Alain Sevin,*† Philippe C. Hiberty,‡ and Jean-Michel Lefour‡

Contribution from the Laboratoire de Chimie Organique Théorique,[1] Batiment F, 75232 Paris Cedex 05, and Laboratoire de Chimie Theorique,[1] Batiment 490, Campus d'Orsay, 91405 Orsay Cedex, France. *Received December 26, 1985*

Abstract: An exploratory study of the reactions arising in the triatomic system Na, F, H has been achieved. In a first step, a complementary use of MO and VB techniques is made for building up correlation diagrams. Special attention was given to the weakly endothermic reaction Na + FH → NaF + H (2), which is shown to proceed through a "harpooning" mechanism in the ground state (GS). For this reaction, a transition state is found at SCF level, but it does not persist when electron correlation is introduced. In the excited state, the presence of stable exciplexes is shown by SCF-CI calculations. For the lowest excited 3P states of Na, the exciplex energy and geometry are close to that of the SCF GS transition state, thus providing a possible reactive channel which links the Na* + FH system to the GS of NaF + H. A small-size VB calculation has been carried out, including the dominant ionic and covalent structures of the aforementioned system, yielding quasi-diabatic and adiabatic potential energy surfaces. These various types of surfaces are analyzed in detail for the harpooning process (reaction 2, GS). They give a clear numerical insight to this mechanism, which essentially results from the crossing between the covalent Na···FH surface and the ionic one $Na^+ \cdots FH^-$.

The gas-phase reactions of alkali metal atoms with small molecules constitute a vast field of investigation for both experimentalists and theoreticians. In this perspective, Li and Na are good candidates for detailed analysis, and many collisional studies of these elements with diatomic molecules have been achieved. Most of these triatomic systems deal with the metal in its ground state (GS) and a nonpolar molecule. Polar molecules, such as hydrogen halides, have been used only scarcely. The prototype system, Li + FH, has been the subject of experimental[2-4] and theoretical studies, either at the semiempirical[5-10] or ab initio + CI level.[11-14] In the case of Na + HX, (X = F, Cl), only a few studies have appeared[3,15] for the GS of the system, but neither an experimental nor a theoretical study of the excited-state reactivity is available. However, the reactions of Na (GS or excited

† Laboratoire de Chimie Organique Théorique.
‡ Laboratoire de Chimie Theorique.

(1) Both laboratories form the UA No. 506 of the C.N.R.S.
(2) Becker, C. H.; Casavecchia, P.; Tiedemann, P. W.; Valentini, J. J.; Lee, Y. T. *J. Chem. Phys.* **1980**, *73*, 2833-2850.
(3) Bartoszek, F. E.; Blackwell, B. A.; Polanyi, J. C.; Sloan, J. J. *J. Chem. Phys.* **1981**, *74*, 3400-3410 and references cited therein.
(4) Raghavan, K.; Upadhyay, S. K.; Sathyamurthy, N.; Ramaswamy, R. *J. Chem. Phys.* **1985**, *83*, 1573-1577.
(5) Zeiri, Y.; Shapiro, M. *Chem. Phys.* **1978**, *31*, 217-237.
(6) Shapiro, M.; Zeiri, Y. *J. Chem. Phys.* **1979**, *70*, 5264-5270.
(7) Zeiri, Y.; Shapiro, M.; Pollak, E. *Chem. Phys.* **1981**, *60*, 239-247.
(8) Walker, R. B.; Zeiri, Y.; Shapiro, M. *J. Chem. Phys.* **1981**, *74*, 1763-1769.
(9) Alvarino, J. M.; Cassavecchia, P.; Gervasi, O.; Lagana, A. *J. Chem. Phys.* **1982**, *77*, 6341-6342.
(10) Lagana, A.; Hernandez, M. L.; Alvarino, J. M. *J. Mol. Struct. (THEOCHEM)* **1984**, *107*, 87-89.

0002-7863/87/1509-1845$01.50/0

Table I. Optimized Geometries and Energies of the Various Molecules, Systems, and SCF Transition States Involved in Linear Reactions 2, 3, and 4[a]

system	SCF (au)	geometry	SCF–CI (eV)
H	−0.498 233		
F	−99.366 689		
Na	−161.841 415		exptl. 3S 0.00; 3P 2.10; 4S 3.19; 4P 3.75; 5P 4.34[c]
FH[b]	−100.022 879	F···0.9016···H	exptl bond energy 5.90
NaF[b]	−261.320 510	Na···1.9282···F	exptl bond energy 4.98
NaH[b]	−162.372 697	Na···1.9130···H	exptl bond energy 2.08
Na/FH	−261.858 315 (0.00)[e]	Na···5.0···F···0.9016···H	GS $1\Sigma^+$ −261.998 122 = 0.00;[d] $2\Sigma^+$ 1.96; 1Π 2.03; $3\Sigma^+$ 3.33; $4\Sigma^+$ 3.61; 2Π 3.74
NaF/H	−261.813 195 (1.23)	Na···1.9282···F···4.0···H	$1\Sigma^+$ 1.36; $2\Sigma^+$ 5.02; $3\Sigma^+$ 5.06; 1Π, $4\Sigma^+$ >7.20
NaH/F	−261.738 150 (3.27)	Na···1.913···H···5.0···F	$1\Sigma^+$ 3.86; $2\Sigma^+$ >6.20
[Na···F···H]*	−261.791 877 (1.81)	Na···1.93···F···1.417···H	$1\Sigma^+$ 1.73; $2\Sigma^+$ 3.12; 1Π 4.36; $3\Sigma^+$ 5.08; $4\Sigma^+$ 5.35; 2Π 5.69
[Na···H···F]*	−261.738 660 (3.26)	Na···1.921···H···1.8362···F	$1\Sigma^+$ 3.47; $2\Sigma^+$ 5.41; 1Π 6.73; $3\Sigma^+$ 7.00
[H···Na···F]*	−261.735 930 (3.33)	H···1.925···Na···3.15···F	$1\Sigma^+$ 3.26; $2\Sigma^+$ >10.0
Na···FH	−261.862 040 (−0.10)	Na···2.3···F···0.9016···H	$1\Sigma^+$ −0.08; $2\Sigma^+$ 1.57; 1Π 1.60; $3\Sigma^+$ 2.41; $4\Sigma^+$ 2.90; 2Π 2.92

[a] The reference energy at SCF + CI level is that of Na + HF at 5 Å (−261.998 122 au). [b] Closed-shell Hamiltonian. [c] Relative energies. [d] Reference energies for the reaction coordinate. [e] Relative SCF energies in eV.

states) with HX constitute a challenge for the theoreticians, because, despite its small size, this system presents several fundamental problems. A first series of questions arises from the fact that the reactive processes occur through very important electronic rearrangements, whose description, in terms of potential energy surfaces (PESs), is complex. Adiabatic PESs, resulting from the avoided crossings of covalent and ionic diabatic surfaces, are expected, thus leading to technical computation difficulties. A second type of question has to be answered regarding the excited-state reactivity which remains unexplored, and therefore requires an exploratory survey. To be experimentally tested, the latter studies have to take into account several series of states, at least including the low-lying 3P, 4S, and 4P components of Na.

Experimentally, Bartoszek et al.[3] have shown that reactions 1 and 2 are endothermic:

$$HCl\ (v = 1\text{–}4) + Na \rightarrow NaCl + H \qquad (1)$$

$$E^* = 14.2\ \text{kcal mol}^{-1}, \qquad \Delta E_0 = +4.2\ \text{kcal mol}^{-1}$$

$$HF\ (v = 1\text{–}5) + Na \rightarrow NaF + H \qquad (2)$$

$$E^* = 30.0\ \text{kcal mol}^{-1}, \qquad \Delta E_0 = 18.0\ \text{kcal mol}^{-1}$$

(the reported values do not include zero-point energies). For these processes, the collision efficiency is around 1; i.e., vibration is extremely efficient in bringing about reaction. On these grounds, the authors propose a "harpooning model" for the mechanism, in which the reaction occurs through a diabatic switch between the covalent HX (vibrationally excited) + M surface to the ionic one, $HX^- + M^+$. The existence of a weakly bonded linear complex, formed between Na and FH (ΔE = −1.2 kcal mol^{-1}, d(Na···F) = 2.261 Å), has been theoretically determined.[12] This complex, which is weaker than in the Li···FH case (ΔE = −4.2 kcal mol^{-1}, d(Li···F) = 1.94 Å), exhibits charge-transfer character, from the hydride to the metal. Its stability is expected to be dominated by electrostatic and polarization energies. We propose, in this article, a theoretical exploratory study of the Na + FH reactions, in the GS and in the low-lying excited states of Na. It results from the preceding discussion of the GS reaction mechanism that SCF–CI techniques are not well-suited for describing in simple terms the covalent to ionic surface switching. In this perspective a small parallel valence-bond (VB) study has been undertaken. The latter method allows for a much clearer understanding of the PESs nature, and is therefore likely to allow for description of the reaction mechanism, accessible to the experimentalists. The following reactions have been examined:

$$E^* = 30.0\ \text{kcal mol}^{-1}, \qquad \Delta E_0 = 18.0\ \text{kcal mol}^{-1}$$

$$Na + H\text{–}F \rightarrow Na\text{–}H + F \qquad (3)$$

$$F + Na\text{–}H \rightarrow F\text{–}Na + H \qquad (4)$$

Owing to the number of reactions that have been examined, and to the number of states that are involved, we have restricted ourselves in this first attempt to linear reaction paths. Moreover, our aim in this work was also to illustrate the ability of a VB treatment in approaching the diabatic behavior and in explaining the major electronic features.

Methodology

Ab initio SCF–CI calculations were achieved using the GAUSSIAN 76 series of programs[16] in the SCF steps and the CIPSI Møller–Plesset algorithm for the CI.[17] A previously described basis set was used for Na;[18] it consists of 6-31G functions[19] for the 1s to 3p AOs, augmented by three s + p uncontracted diffuse Gaussians of exponents 0.01, 0.0075, and 0.001. This basis set gives good results for the low-lying valence and Rydberg states of the atom. Morevoer, its diffuse part has been adapted for taking into account polarization and charge-transfer effects. The same type of basis set was taken for F: 6-31G for 1s to 2p AOs, augmented by a diffuse s + p set of exponent 0.1076. The standard 6-31G** basis set was used for H. All geometries were optimized, for the lowest state, with a full gradient technique.

The RHF Nesbet Hamiltonian[20] was used throughout. The resulting optimal MOs were used for building the multireference basis of the CI. The Møller–Plesset perturbation calculation was then performed on a reference set ranging from 80 to 150 determinants, yielding about 3 to 4 10^6 perturbative terms. This procedure was repeated at each calculated point of the reaction coordinate (RC), for each type of state symmetry. In Tables I and II are given the optimized geometries and the calculated potential energies of the various molecules, systems, and crucial points of the RCs. Several points are worthy of comment. (i) The SCF energies of the systems composed of a stable molecule (FH, NaH, NaF) and an atom (Na, F, H), respectively, calculated at 4- to 5-Å separation with the open-shell Hamiltonian, are not equal to the sum of the energies of the individual components. The reason is that the energies of the isolated stable molecules have been calculated with the usual closed-shell Roothaan's Hamiltonian,[21] thus yielding a small difference with the energy

(11) Lester, W. A., Jr.; Krauss, M. *J. Chem. Phys.* **1970**, *52*, 4775–4781. Balint-Kurti, G. G.; Yardley, R. N. *Faraday Discuss. Chem. Soc.* **1977**, *62*, 77.
(12) Trenary, M.; Schaefer, H. F., III; Kollman, P. *J. Am. Chem. Soc.* **1977**, *99*, 3885–3886.
(13) Chen, M. M. L.; Schaefer, H. F., III *J. Chem. Phys.* **1980**, *72*, 4376–4393.
(14) Batcha, I. N.; Sathyamurthy, N. *J. Chem. Phys.* **1982**, *76*, 6447–6449.
(15) Heismann, F.; Loesch, H. J. *Chem. Phys.* **1982**, *64*, 43–67.
(16) Peterson, M.; Poirier, R. MONSTERGAUSS, Department of Chemistry, University Of Toronto, Canada, 1981.
(17) (a) Huron, B.; Malrieu, J. P.; Rancurel, P. *J. Chem. Phys.* **1973**, *58*, 5745. (b) Malrieu, J. P.; *Theor. Chim. Acta* **1982**, *62*, 163–174. (c) Evangelisti, S.; Daudey, J. P.; Malrieu, J. P. *Chem. Phys.* **1983**, *75*, 91–102.
(18) Sevin, A.; Chaquin, P. *Chem. Phys.* **1985**, *93*, 49–61.
(19) (a) Francl, M. M.; Pietro, W. J.; Hehre, W. J.; Binkley, J. S.; Gordon, M. S.; De Frees, D. J.; Pople, J. A. *J. Chem. Phys.* **1982**, *77*, 3654–3665. (b) Gordon, M. S.; Binkley, J. S.; Pople, J. A.; Pietro, W. J. *J. Am. Chem. Soc.* **1982**, *104*, 2797–2803. (c) Pietro, W. J.; Francl, M. M.; Hehre, W. J.; De Frees, D. J.; Pople, J. A.; Binkley, J. S. *Ibid.* **1982**, *104*, 5039–5048.
(20) (a) Nesbet, R. K. *Rev. Mod. Phys.* **1961**, *31*, 28; **1963**, *35*, 552. (b) Davidson, E. R. *Chem. Phys. Lett.* **1973**, *21*, 565.
(21) Roothaan, C. C. J. *Rev. Mod. Phys.* **1960**, *23*, 69–89.

Table II. Optimized Geometry of the SCF Bent Transition State for Reaction 2, and Energy Variation of the Na···FH Cluster upon Bending

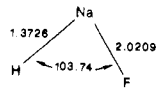

SCF: −261.799 491 au
SCF + CI: −261.948 690 au
relative:[a] 1.34 eV

		energies (eV) bending angle			
		180°	150°	135°	90°
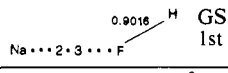	GS	0.0	0.003	0.020	0.162
	1st excited	0.0	−0.050	−0.057	0.155

[a] Relative to Na···5 Å···FH (−261.998 122 au) as in Table I.

obtained for the whole system, with the open-shell Hamiltonian. (ii) The SCF transition-state geometries have been obtained by using a single reference configuration, the GS. They all have a strong negative root in the Hessian matrix. But, at the multireference CI level, the only transition state which subsists is the linear one, found along path 2, the other three geometries corresponding to energies that are below NaH + F, in reactions 3 and 4, and slightly below NaF + H, for the triangular one, in path 2.

The CI energies of the excited states of Na + FH, at a 5-Å distance, are in very good agreement with the asymptotic experimental values.[22] In practice, we have taken these values as an origin of the energies. Even at this distance, the splitting of the P components between Σ^+ and Π states is observed. Two reasons might be invoked for this behavior. The first one results from the fact that the diffuse set of Na orbitals interacts to some extent with FH at this distance. The second is inherent to the perturbative Møller–Plesset calculation which does not involve the same symmetry orbitals for the Σ^+ and the Π states, thus yielding very small energy differences. The difference (0.07 eV for the 3P states) is more pronounced for the 4P states, because the latter have been calculated using the optimal reference set of the 3P components. Therefore, the calculation is slightly less accurate for the states of high energy.

The VB calculations have been performed by using a program written by Flament[23] and one of us (J.M.L.). The steps of the calculation are the following. In the first step, a set of atomic orbitals is obtained by ab initio SCF calculations on each isolated fragment H, F, and Na. For these calculations, the previously described basis set has been used, exclusive of the Rydberg orbitals of Na. In the second step, the one-electron and two-electron atomic integrals are computed at each point of the RC and then transformed on the SCF fragment orbitals. Each VB configuration is expressed as a linear combination of Slater determinants which are constructed from these fragment SCF orbitals. It is worth noting that these orbitals become nonorthogonal when the atoms are brought together. In the last step, we first define optimized structures (OS) that are variationally determined linear combinations of either covalent (Heitler–London) or ionic VB configurations, and that each represent a given purely covalent or purely ionic bonding scheme (see Table III). Then, by variationally combining both types of OS, we build VB wave functions (VBWF), in such a way that each of them represents a bonding scheme in which each bond has an optimal ratio of ionic vs. covalent components. Strictly speaking, these VBWFs are not true diabatic states, since they do not satisfy the ($<\Phi_i|\delta/\delta Q|\Phi_j> = 0$) condition. For this reason, they can be regarded as quasi-diabatic wave functions.

The computation of the Hamiltonian matrix elements between nonorthogonal determinants is performed using the Prosser and Hagstrom[24] transformation for calculating the minors of the overlap matrix. This results in important savings in computing time.[25]

Diabatic MO Correlations

Prior to a detailed study of the PESs, it is worth outlining the major electronic events taking place in reactions 2, 3, and 4. For the sake of simplicity, let us define the "active" MOs according

Table III. VB Configurations Needed To Describe the Various Types of Bond which Can Be Formed in Reactions 2, 3, and 4, with Their Coefficients in Each Optimized Structure[a]

optimized structures	VB configurations	coefficients
H	h	1
Na	$(Na_{core})^2Na_{3s}$	1
F	$(F_{1s}F_{2s}F_{2p_x}F_{2p_y})^2F_{2p_z}$	1
H–F	$(F_{1s}F_{2s}F_{2p_x}F_{2p_y})^2F_{2p_z}$ h	0.60
	$(F_{1s}F_{2s}F_{2p_x}F_{2p_y})^2F_{2p_z}$ h′	0.08
	$(F_{1s}F_{2s}F_{2p_x}F_{2p_y})^2F_{2p_z}$ h″	0.19
H^+F^-	$(F_{1s}F_{2s}F_{2p_x}F_{2p_z})^2(F_{2p_z})^2$	0.47
	$(F_{1s}F_{2s}F_{2p_x}F_{2p_z})^2F_{2p_z}F_{2s}$	0.08
	$(F_{1s}F_{2s}F_{2p_x}F_{2p_z})^2F_{2p_z}F_{2s'}$	0.05
H–Na	$(Na_{core})^2Na_{3s}$ h	0.46
	$(Na_{core})^2Na_{3p_z}$ h	0.05
	$(Na_{core})^2Na_{3s'}$ h	0.12
	$(Na_{core})^2Na_{3p_z'}$ h	0.14
H^-Na^+	$(Na_{core})^2$ h^2	0.48
	$(Na_{core})^2$ h h′	0.21
	$(Na_{core})^2$ h h″	0.06
Na–F	$(Na_{core})^2(F_{1s}F_{2s}F_{2p_x}F_{2p_y})^2Na_{3s}F_{2p_z}$	0.22
	$(Na_{core})^2(F_{1s}F_{2s}F_{2p_x}F_{2p_y})^2Na_{3s'}F_{2p_z}$	0.06
	$(Na_{core})^2(F_{1s}F_{2s}F_{2p_x}F_{2p_z})^2Na_{3p_x}F_{2p_x}$	0.18
	$(Na_{core})^2(F_{1s}F_{2s}F_{2p_x}F_{2p_z})^2Na_{3p_x'}F_{2p_x}$	0.15
	$(Na_{core})^2(F_{1s}F_{2s}F_{2p_y}F_{2p_z})^2Na_{3p_y}F_{2p_y}$	0.18
	$(Na_{core})^2(F_{1s}F_{2s}F_{2p_y}F_{2p_z})^2Na_{3p_y'}F_{2p_y}$	0.15
Na^+F^-	$(Na_{core})^2(F_{1s}F_{2s}F_{2p_x}F_{2p_y})^2(F_{2p_z})^2$	0.75
	$(Na_{core})^2(F_{1s}F_{2s}F_{2p_x}F_{2p_y})^2F_{2p_z}F_{2p_z'}$	0.16
	$(Na_{core})^2(F_{1s}F_{2s}F_{2p_x}F_{2p_y})^2F_{2p_z}F_{2p_z''}$	0.12

[a] (Na_{core}) stands for $(Na_{1s}Na_{2s}Na_{2p_x}Na_{2p_y}Na_{2p_z})$; h, h′, and h″ are s-type orbitals of the hydrogen atom. The primed and double-primed orbitals are those which are virtual in the SCF calculations of the fragment orbitals.

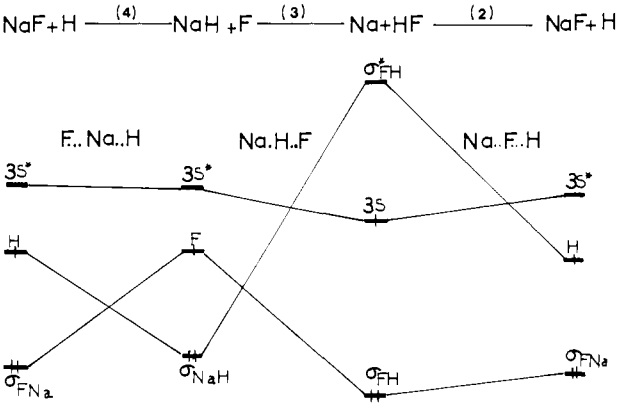

Figure 1. Diabatic MO correlations for reactions 2, 3, and 4.

to the schematic view of Figure 1. On purpose the various MOs that do not directly intervene in the bonds that are broken or formed have been omitted. For each reaction, it is assumed that the diatomic moiety, i.e., H–F, F–Na, or H–Na, is characterized by a couple of bonding and antibonding levels, σ and σ^*, respectively. Considering the relative electronegativity of the partners, and using elementary perturbation theory arguments, it follows that (i) in the bonding σ MO, the dominant contribution comes from the most electronegative element, so that the latter is surrounded by the largest part of the electronic density; (ii) a symmetrical argument can be used for the antibonding σ^* MO that has a leading contribution from the less electronegative element. Similarly, the 3S level of Na, being occupied by an unpaired electron in the atomic GS, is labeled 3S* when it is a component of H–Na or F–Na. In both cases, it constitutes the essential contribution to a low-lying antibonding (or nearly nonbonding) MO. Following the natural orbital correlation principles,[18,26] we now define the natural MO correlations as those preserving the leading character of each level. In other words,

(22) Moore, C. E. Atomic Energy Levels, National Bureau of Standards: Washington, D.C.: Vol. I, 1949; Vol. II, 1952.
(23) Flament, J. P. Laboratoire de Synthèse organique, Ecole Polytechnique, 91120 Palaiseau, France.
(24) Prosser, F.; Hagstrom, S. *Int. J. Quantum Chem.* **1967**, *1*, 88; *J. Chem. Phys.* **1968**, *48*, 4807.
(25) For recent papers on the evaluation of cofactors, see: (a) Leasure, S. C.; Balint-Kurti, G. G. *Phys. Rev. A* **1985**, *31*, 2107. (b) Hayes, I. C.; Stone, A. J. *Mol. Phys.* **1984**, *53*, 69. (c) Figari, G.; Magnasco, V. *Ibid.* **1985**, *55*, 319.
(26) Devaquet, A.; Sevin, A.; Bigot, B. *J. Am. Chem. Soc.* **1978**, *100*, 2009.

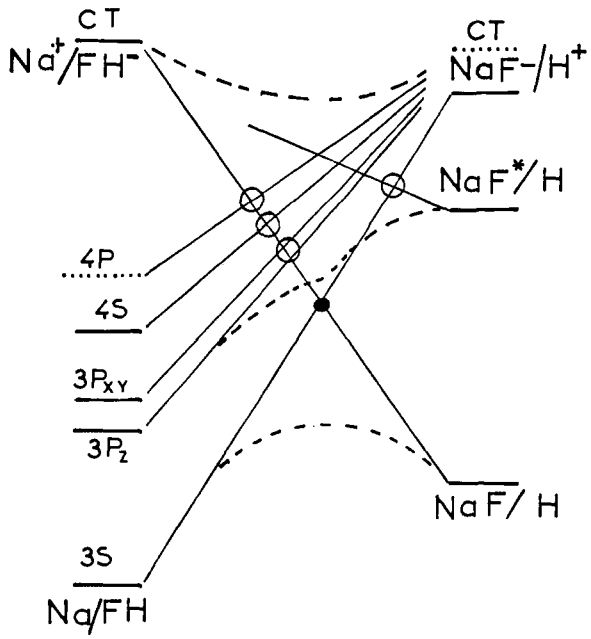

Figure 2. State correlations for reaction 2.

this means that the electrons remain located on the atomic fragment around which they are initially concentrated. Indeed, this is nothing but a pictorial way of looking at the major changes occurring at very polar bonds. However, these correlations allow for simply describing the initial (or quasi-diabatic) behavior of the various systems under scrutiny, and we will see in coming sections that this point of view is very close to a VB analysis. It is clear that in real processes, adiabatic PESs involving smoother electronic changes will result from taking into account the role of the other electrons of the system. These concepts will now be applied to the study of reactions 2, 3, and 4. For the sake of simplicity, we have restricted ourselves to limiting linear reaction paths, which clearly allows for underlining the major electronic events.

(A) Reaction 2: H-F + Na → Na-F + H. In the right part of Figure 1 we see that σ_{FH} and σ_{FNa}, both having strong F character, are directly correlated. The 3s AO of Na is correlated with its counterpart, 3s* in Na-F. The valence AO of H, which bears the unpaired electron in the final system, is correlated with σ^*_{FH}, where the hydrogen contribution dominates. A MO crossing results which, in turn, will be adiabatically avoided at SCF level. This crossing is likely to induce the existence of a potential energy barrier along the GS PES. It reveals that the electronic configuration of the reactants which is linked to the products is a charge transfer Na^+/FH^-.

(B) Reaction 3: Na + H-F → Na-H + F. σ_{FH} is correlated with the orbital bearing the unpaired electron of F*; 3s of Na is correlated with 3s* in Na-H. The bonding σ_{NaH} MO, where H character is dominant, is correlated with σ^*_{FH}. The overall electronic rearrangement is more complex than in reaction 2. The GS electronic configuration of Na-H + F is naturally correlated with a charge-transfer configuration: $(\sigma_{FH}{}^1(3s)^0(\sigma^*_{FH})^2$. The latter moiety now corresponds to an excited state of FH^-, i.e., $Na^+/(FH^-)^*$.

(C) Reaction 4: F + Na-H → F-Na + H. The MO correlations are straightforwardly obtained. σ_{NaH} is correlated with the atomic AO of H* bearing the unpaired electron; σ_{FNa} is correlated with the atomic AO of F*, and 3s* of Na-H is correlated with 3s* of Na-F, both having a dominant 3s character. Here again we see that the GS electronic configurations of the reactants and the products are not directly linked, but involve the crossing of charge-transfer configurations: $NaH/F^* \leftrightarrow NaF^+/H^-$ and $NaF/H^* \leftrightarrow NaH^+/F^-$.

In all cases, the MO crossings only adequately describe the behavior of the GS of the system. We have not drawn the correlations of low-lying levels such as 3p, 4s, and 4p of Na, for example. The corresponding MO correlation topology does not deserve comment, and it is likely to be rather flat, since, in each case, these levels do not appreciably play a role in the bonding or antibonding valence pattern. However, their presence will be very important for building the related state correlations.

State Correlations for Reaction 2: Na + F-H → Na-F + H

Let us focus our attention on this reaction which is the only feasible one, being either weakly endothermic in the GS, or exothermic in the excited state. In a linear, $C_{\infty v}$ geometry, the degeneracy of the 3P and 4P states of Na is split, yielding $3P_z$, $4P_z$ (Σ^+ symmetry), on the one hand, and $3P_x + 3P_y$, $4P_x + 4P_y$ (Π symmetry), on the other hand. The state correlations of the reactants' and products' GS directly result from the preceding discussion of MO correlations. Both are correlated with charge transfers, and the resulting crossing is materialized by a full circle. These correlations clearly show the fundamental role of the ionic species FH^- and NaF^-. Theoretical studies have shown that FH^- is not stable at the equilibrium distance of the uncharged molecule,[27,28] while NaX^- or LiX^- remain stable in the same conditions.[29-33] But, by approaching a cationic counterion, both (Na^+, FH^-) and (H^+, NaF^-) systems become attractive, and, therefore, the corresponding correlations are assumed to have monotonous exothermic slopes, as shown in Figure 2. Moreover, we are mainly interested in the initial gradient of GS quasi-diabatic PESs of reactants and products since it is likely to rule to a large extent the shape of the actual adiabatic potential energy barrier, at the extremities of the reaction coordinate. The correlations of the excited states of Na may be easily obtained by using in a first step the terminology of Figure 1, and replacing the "3S" label by 3P, 4S, or 4P. To a first-order approximation, the energies of these states depend on the energy gap separating 3S from the considered component, so that their initial behavior will remain parallel to that of the GS of the system. All these states are correlated with excited states of the polar final system, according to the scheme, $Na^{*\bullet}/FH \leftrightarrow (NaF)^{*-}/H^+$, where the asterisk means that the unpaired electron is located on a diffuse MO, keeping the same Na character throughout the process. The first excited state of NaF is found at high energy (see Table I), and its correlation toward a high-energy charge transfer of the reactants is indicated. All the excited-state correlations cross the quasi-diabatic correlations of the GS of reactants and products, as shown by open circles. A great number of adiabatic avoided crossings take place for the states of Σ^+ symmetry, and the nature of the resulting low-lying adiabatic PESs will reflect this complex mixing pattern.

This schematic diagram reveals that the adiabatic nature of the low-lying PESs differs in the vicinity of the poles of the system. Around Na + FH, several low-lying excited states interfere with the quasi-diabatic dissociative charge-transfer surface, and, therefore, the system possesses some opportunity of progressively adapting itself to the overall electronic changes. This kind of screening effect is no longer possible around NaF + H, where no low-lying excited state is available. On these grounds, a transition state is found between Na + FH and NaF + H. This statement, which is verified at SCF level (Tables I and II), is not in contradiction with the fact that, at large CI level, the barrier disappears in the triangular geometry. The latter arguments show that, even in that case, important electronic rearrangements occur in this region of the RC.

(27) Bondybey, V.; Pearson, P. K.; Schaefer, H. F., III *J. Chem. Phys.* **1972**, *57*, 1123-1128.
(28) Griffing, K. M.; Kenney, J.; Simons, J.; Jordan, K. D. *J. Chem. Phys.* **1975**, *63*, 4073-4075.
(29) Jordan, K. D.; Griffing, K. M.; Kenney, J.; Andersen, E. L.; Simons, J. *J. Chem. Phys.* **1976**, *64*, 4730-4740.
(30) Jordan, K. D.; Luken, W. *J. Chem. Phys.* **1976**, *64*, 2760-2766.
(31) Rosmus, P.; Meyer, W. *J. Chem. Phys.* **1978**, *69*, 2745-2751.
(32) Jordan, K. D.; Wendoloski, J. J. *Mol. Phys.* **1978**, *35*, 223-240.
(33) (a) Karo, A. M.; Gardner, M. A.; Hiskes, J. R. *J. Chem. Phys.* **1978**, *68*, 1942-1950. (b) Stevens, W. J.; Karo, A. M.; Hiskes, J. R. *Ibid.* **1981**, *74*, 3989-3998.

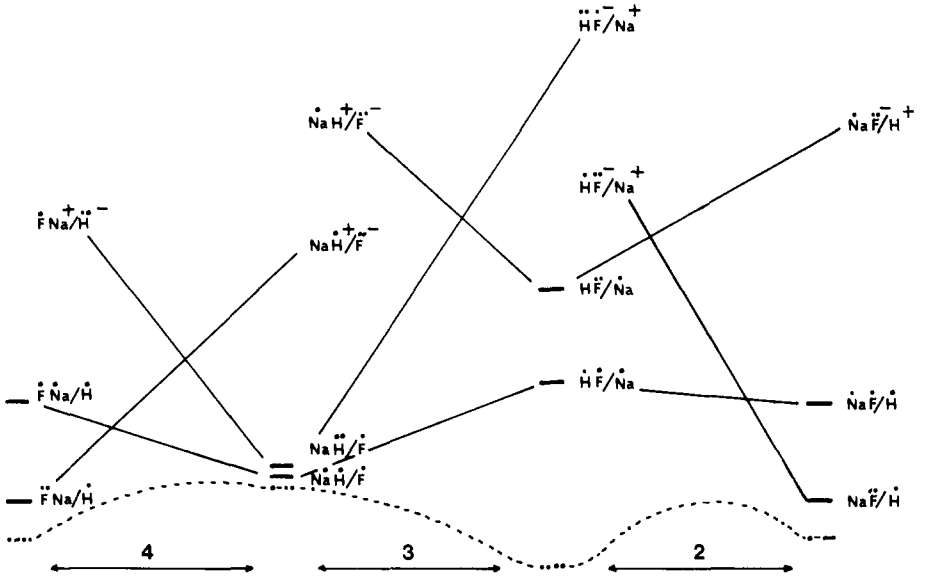

Figure 3. Quasi-diabatic (full lines) and adiabatic (dotted lines) VB correlations for reactions 2, 3, and 4. Only the low-energy optimized structures, materialized by a thick stroke, have been effectively computed.

VB Correlations of Optimized Structures

The analysis of VB correlations provides an original alternative way of looking at the complex interplay between covalent and ionic structures along the reaction path. In order to be of simple and general use, the corresponding diagrams have to fulfill two criteria: (i) to contain the maximum qualitative chemical information that can be obtained without heavy calculations, and (ii) to provide us with an estimation of the energetics of the process, especially of the various potential energy barriers. The elaboration of a strategy deserves comment. In a first step, it will be illustrated by examples taken from the model study of reaction 2.

(A) Reaction 2. A small-dimension VB calculation (see the Methodology section and Table III) was performed on the isolated molecules FH and NaF, including the ionic and covalent configurations. We thus obtained the energies of both types of optimized structures, and the energy of their optimal mixing, after diagonalization of the interaction matrix. For example, the covalent OS of the reactants, whose shorthand notation is $\dot{H}-\dot{F}/\dot{N}a$, has the energy of the covalent OS H–F augmented by that of the isolated Na atom. We then place these OSs by order of increasing energy and we correlate the OSs of identical electron localization, as displayed in full lines in Figure 3. This procedure yields two kinds of information. The first is the topology of the various crossings occurring between covalent and ionic surfaces; the second is a qualitative hierarchy of these crossings. We see that, along the reaction path, a crossing between the covalent surface, $\dot{H}\ \dot{F}\ \dot{N}a$, and the ionic one, $Na\ \ddot{F}\ \dot{H}$, occurs at low energy. Therefore, this crossing is very likely to play a fundamental role in the electronic mechanism. This is indeed the translation, into electronic language, of the so-called "harpooning" model. At higher energy another crossing occurs between $H\ \ddot{F}\ \dot{N}a$ and the charge-transfer $\dot{H}\ \ddot{F}\ Na$. Starting from Na + FH, we have a sequence of electronic events: (i) the covalent OS is diabatically linked to its counterpart in the products; (ii) the ionic OS of FH is not diabatically linked to the low-lying ionic OS of NaF, and the nonmonotonous correlation requires a surface switching with the charge-transfer surface. At this stage of our analysis, nothing more can be said, either regarding the actual thermodynamics of the reaction, or regarding the existence, or not, of a potential energy barrier. A misleading conclusion even might arise from the consideration that both $\dot{N}a\ddot{F}/\dot{H}$ and $Na\ddot{F}/\dot{H}$ lie below $\dot{H}\ddot{F}/\dot{N}a$. The reason is that the relative energies of the various VB optimized structures do not presume the energy of their optimal linear combination, and only allow for the elucidation of the crossing topology. The latter point is illustrated by the bottom part, in broken lines, where we have reported the energies of the optimal HF/Na and NaF/H VBWFs, after mixing of ionic and covalent components (the latter procedure is equivalent to a 2 × 2 CI). Because of the short HF distance, a very important overlap between covalent and ionic OSs exists, thus giving an important interaction term (off-diagonal element), and, finally, an important stabilization with respect to the original OSs. The corresponding stabilization is much smaller in NaF, so that the thermodynamic balance is correctly restored after this step. Starting from the right, i.e., NaF + H, we see that at the beginning of the RC, the optimal solution, which is quite close to $Na\ddot{F}/\dot{H}$, will follow its behavior to a large extent, thus driving the system toward high energy. Then, the crossing with the covalent surface will take place and finally the system will reach the final situation. As in the preceding discussion of state correlations, the existence of a transition region is predicted.

(B) Reaction 3. Using the same types of arguments as in dealing with reaction 2, two important points emerge. The first is that the covalent OSs are monotonously linked, without crossing with ionic ones. The second is that upon mixing of ionic and covalent OSs of NaH very little stabilization results. On going from NaH/F to NaF/H (left to right), we see that the reaction profile will be dominated by the monotonous covalent correlation, in such a way that little or no barrier is predicted along the exothermal path.

(C) Reaction 4. Starting from NaH/F (right to left), we see that the crossing topology is similar to that of reaction 2. The lowest energy surface follows the covalent curve which is rising slowly because both $\dot{N}a\ \dot{F}/\dot{H}$ and $\dot{N}a\ \dot{H}/\dot{F}$ covalent OSs lie in low-energy regions; then the adiabatic curve must go down early to reach the energy of the products, which is lower than that of the reactants. Therefore, the barrier may be predicted to be rather small.

SCF–CI Potential Energy Surfaces for Reaction 2

The calculated SCF–CI PESs for reaction 2 are given in Figure 4. The exploration of the optimized GS RC reveals three typical regions of the RC. Starting from Na + FH at infinite separation we first observe during the approach a splitting of the 3P levels of Na, which is more pronounced for the levels of high quantum number, four or five. In our drawing, the origin of the abcissa has been taken at a Na···FH distance of 5 Å.

(A) Region I of the RC: Formation of a Cluster and of Exciplexes. In the ground state, this region corresponds to a linear approach of the reactants, practically without geometry relaxation of FH. A weakly attractive cluster is found at 2.3 Å which is only 0.08 eV more stable than the isolated components. As already shown in Table II, the deviation from linearity is weakly endothermic. An important difference arises in the excited states:

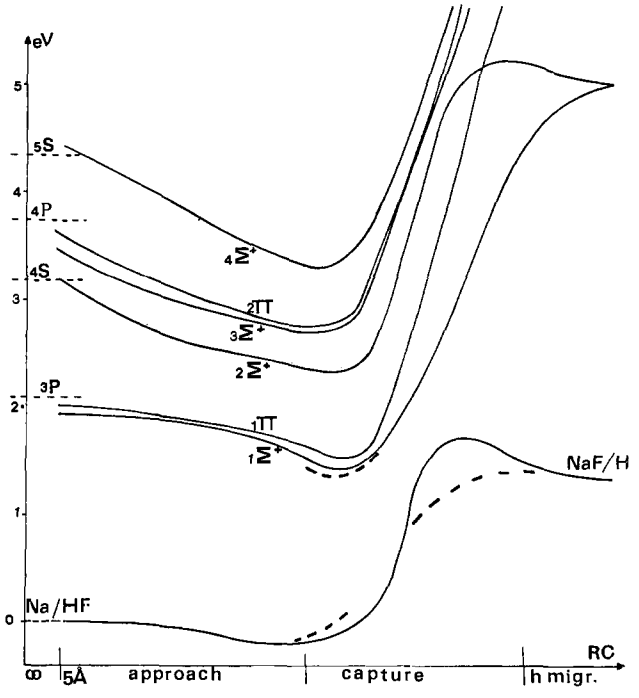

Figure 4. Calculated SCF–CI potential energy surfaces for reaction 2. The solid lines display the potential energy curves for the linear pathway; the dashed lines correspond to optimally bent pathways (see text).

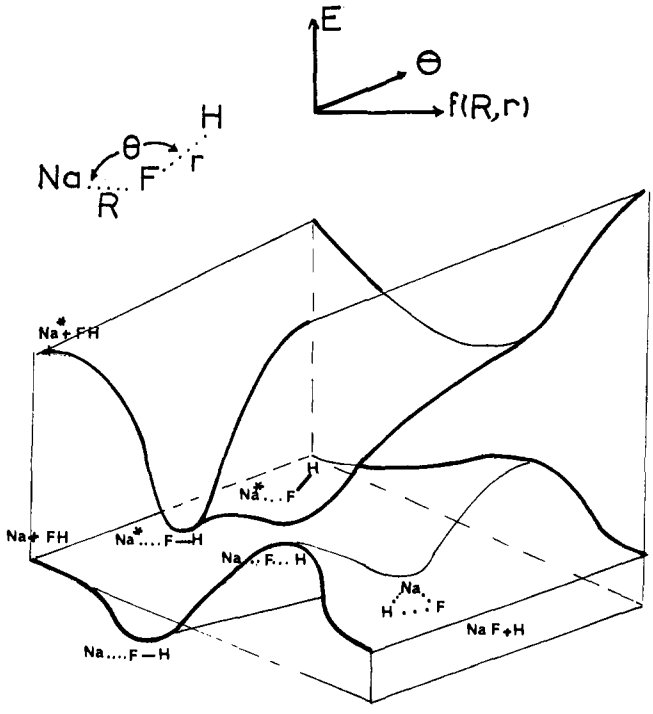

Figure 5. Schematic view of the lowest two surfaces for reaction 2. The reaction coordinate $f(R,r)$ is the same as the one previously discussed in Figure 4.

stable exciplexes result from the approach, the corresponding potential energy wells being around 0.5 eV for the 3P states, and more than 1 eV for the more diffuse states. Dealing with the lowest excited state, the potential energy varies very smoothly around the optimal geometries. In other words, the corresponding atom + molecule complexes are not very directional. They result from back-donation from the F lone pairs to the empty 3p orbitals of Na. The latter fact is corroborated by the finding that in reaction 3, where H approaches Na, no such cluster or exciplexes are found.

(B) Region II of the RC. This region corresponds to the reaction process itself. First of all we see that, starting from the GS cluster, an endothermic process leads to the saddle point, and then to NaF + H. This endothermic behavior is much more pronounced in the excited states, where very steeply ascending PESs are obtained, which are linked to the high-energy excited states of NaF + H. It is worth comparing the constrained linear transition-state geometry, Na···1.93···F···1.47···H, with that of the saddle point displayed in Table II. In the linear geometry, the Na···F distance is quite equal to the resting GS geometry of isolated NaF (1.928 Å) while it is longer in the bent form, 2.02 Å. This means that the reverse spontaneous reaction, i.e., NaF + H → Na + FH, occurs through a region which corresponds to the SCF saddle point, which is less "reactant-like" than in the linear path, according to the Bell–Evans–Polanyi principle terminology,[34] also refered to as Hammond's postulate.[35] Dealing with the excited-state reactivity, it is worth noting that either the bent SCF saddle point or linear transition-state regions are at slightly lower energies than the 3P excited state, at infinite separation, and in close vicinity to the corresponding exciplex. This quasi-contact allows for a possibility of switching from the exciplex surface to the GS one, through coupling of the atomic motion with the electronic wave function. The nonvanishing matrix element that couples both surfaces, of general form, $\langle\psi_{GS}|\delta/\delta_q|\psi_{3P}\rangle$, must have the Σ^+ or A′ symmetry in the linear or bent geometry, respectively, so that only two components of 3P might be reactive.[36] However, the best probability of surface switching occurs in the neighborhood of the constrained linear GS saddle point, since, on the one hand, the gap between the GS and the first excited state is minimum, and, on the other hand, the latter state is only weakly stabilized through bending. If, starting from the excited surface the system reaches the GS surface, as schematically displayed in Figure 5, two important points emerge: (i) the overall process is exothermic, and its feasibility is important, owing to the quasi-contact in the switching region; (ii) the corresponding energy excess will be distributed among the fragments, H being expelled with a noticeable kinetic energy, FH possessing an important vibrational + rotational excitation.

There is no adiabatic reactive channel for the excited states of higher energy, either in forward or reverse reactions. The behavior of the 4(S + P) and 5(S + P) states deserves comment. These states are trapped in potential energy wells where one possible evolution consists in fluorescing towards the GS with an important red shift. Through nonradiative evolution, the redistribution between kinetic and vibrational energy remains to be evaluated. Because of its strong cohesion (ν_0 = 4138 cm^{-1}, F = 9.6 mdyn/Å), on the one hand, and because its asymptotic limit is very high (F + H at 5.81 eV), on the other hand, FH is not likely to thermally dissociate in the absence of strong coupling with Na. Since the latter is only weakly bonded to FH in the GS cluster, we might qualitatively assess that this kind of deactivation will only be poorly reactive. The possibilities of diabatic couplings between 4(S + P) and 5(S + P) states with the ionic dissociative states, Na^+/FH^-, remains to be examined. There exists an analogy between a Rydberg state of high quantum number of Na, which can be regarded as an electron gravitating far from a positively

(34) A clear discussion of these ideas is found in: Dewar, M. J. S.; *The MO Theory of* Organic *Chemistry*; McGraw-Hill: New York, 1969; p 284. A recent survey is found in: Pross, A.; Shaik, S. S. *Acc. Chem. Res.* **1983**, *16*, 363–370.

(35) Hammond, G. S. *J. Am. Chem. Soc.* **1955**, *77*, 334. See the discussion by: Salem, L. In *Electrons in Chemical Reactions: First Principles*; Wiley: New York, 1982; p 49.

(36) Lorquet, J. C.; Lorquet, A. J.; Desouter-Lecomte, M. *Quantum Theory of Chemical Reactions*, Reidel, D.: Dordrech, Holland, 1980; Vol. 2, p 241 and references cited therein. See also: Desouter-Lecomte, M.; Leyh-Nihant, B.; Praet, M. T.; Lorquet, A. J.; Lorquet, J. C. *J. Phys. Chem.* **1985**, *89*, 214–222.

(37) Herzberg, G. *Molecular Spectra and Molecular Structure I Spectra of Diatomic Molecules*; Van Nostrand, D.: Princeton, N. J., 1950. Theoretical value: Gaw, J. F.; Yamaguchi, Y.; Vincent, M. A.; Schaefer, H. F., III *J. Am. Chem. Soc.* **1984**., *106*, 3133–3138.

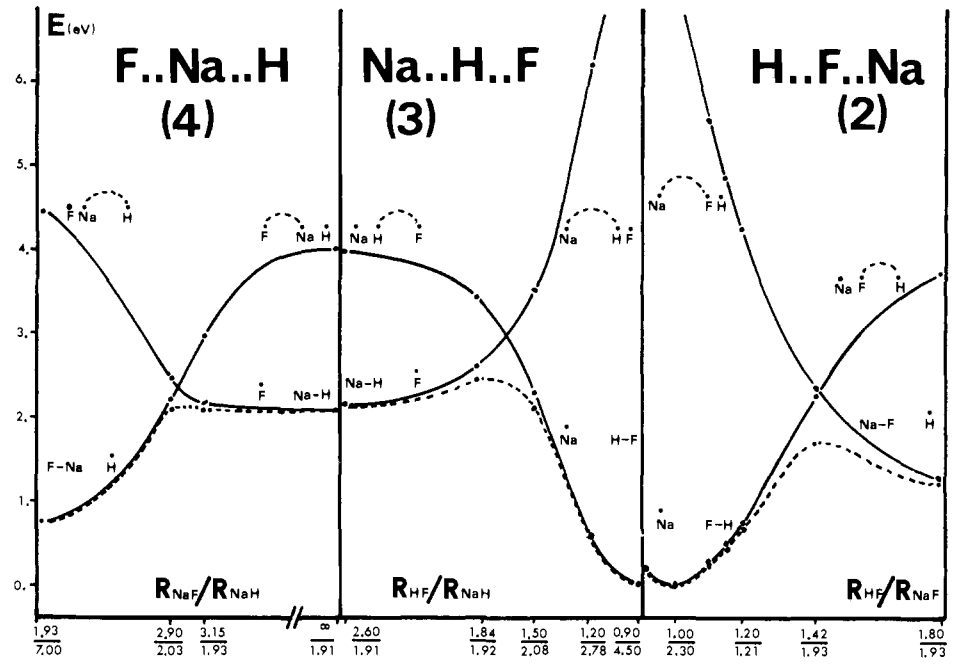

Figure 6. Calculated Shaik's diagrams for reactions 2, 3, and 4. Each solid line represents the energy of a VBWF as a function of the geometric deformation of the supersystem. In each VBWF, the atom topped by a dot is left uncoupled, while the two other atoms are coupled in a covalent and/or ionic manner. For each reaction, the length of the strongest bond is chosen as the RC and the remaining bond length is optimized. Both lengths are indicated in the abcissa, in Å. The reference absolute energy (0 eV) is −261.834 54 au, and corresponds to the (HF···Na) cluster.

charged core, and the charge-transfer complex. In both cases, a strong electrostatic attraction is found, but the difference comes from the localization of the unpaired electron. Owing to their diffuseness, the Rydberg states largely overlap with FH in the complex. Moreover, we have seen that the partial conjugation between F and Na decreases the electronic density around F, in the complex. All these factors act in rendering the electron transfer quite easy, and we therefore might expect the diabatic coupling between the Rydberg states and the dissociative PES to be significant, leading to potentially reactive channels. At this level of investigation, nothing can be said about the actual efficiency of such diabatic pathways. We only can conclude that the resulting NaF + H system would be hot, bearing a large excess of translational energy, essentially stored in H, and vibrational and rotational energy, in NaF.

Valence-Bond Energy Profiles for Reactions 2–4

To better illustrate the mechanisms of reactions 2–4, we have investigated some of their potential energy surfaces by means of VB calculations, using the method described above. In this exploratory attempt, we have restricted ourselves to the analysis of linear geometries. Taking reaction 2 as an example, one quasi-diabatic energy curve represents the energy of the H–F/Na VBWF, i.e., the result of a nonorthogonal configuration interaction (CI) involving all the VB configurations in which H is bonded to F, in an ionic or covalent manner, while Na is left uncoupled. The ionic vs. covalent ratio of the HF bond is therefore variationally optimized, and thus depending on the H–F bond length. For example, when H and F are far from each other, the H–F linkage is best described as a singlet-coupled diradical (upper right-side solid curve) and is thus entirely covalent in the Na/F–H VBWF, while it has both ionic and covalent components at the bond stage when F and H are close to each other (lower left-side solid curve). The other quasi-diabatic curve represents the H/F–Na VBWF, and the adiabatic curve is the result of a general CI involving all H/F–Na and H–F/Na types of structures. If enough VB configurations are involved in this latter CI, the adiabatic curve calculated this way must in principle be quantitative and reproduce the energetics of our MO + large-scale CI computation. However, our purpose in applying the VB method was mainly illustrative, and we used a very small number of configurations, yet sufficient to get correct orders of magnitudes, comparable to those obtained at the SCF level. As an example, the H–F bond is described by six VB configurations, and the HNa and NaF bonds by seven and nine, respectively (see Table II).

It should be noted that the VB diagrams discussed in this section differ in nature from those displayed in Figure 3. Here, each quasi-diabatic curve represents a given way of coupling the electrons, the ionic:covalent ratio of this coupling being optimum. In Figure 3, on the other hand, optimized structures of identical electron localization are correlated, whatever the way these electrons may be coupled.

The results for reactions 2–4 are displayed in Figure 6. It is interesting to comment the behavior of the quasi-diabatic curves of, e.g., reaction 2. The left side of the diagram corresponds to the following geometry of the supersystem: F–H has its equilibrium bond length and Na is separated from F by 2.35 Å. Therefore, the Na/F–H VBWF is in its equilibrium geometry and is low in energy. On the other hand, at the same geometry of the supersystem, the Na–F/H VBWF is high in energy, since it represents a stretched Na–F bond. As one moves along the reaction coordinate, i.e., from the left side to right side of the diagram, the F–H bond length increases while the Na–F one decreases up to its equilibrium value. Consequently, the F–H/Na energy curve goes up while the Na–F/H one goes down, and both curves cross somewhere in the diagram. If we now allow some mixing between both curves, by performing a nonorthogonal CI involving all VB configurations, we get the adiabatic curve. It should be noted that, at each end of the diagram, the adiabatic curve is merged with a quasi-diabatic one. This is because the mixing between both curves is very small in these geometries, since the energy gap between quasi-diabatic curves is large.

Shaik has recently developed a theory[38-40] in which the activation barriers of reactions are considered as the results of avoided crossings of VBWF energy curves of VB type, as the ones displayed in Figure 6. The power of this theory lies in the fact that the

(38) Shaik, S. S. *J. Am. Chem. Soc.* **1981**, *103*, 3692.
(39) (a) Shaik, S. S. *Nouv. J. Chim.* **1982**, *6*, 159; (b) Shaik, S. S. *Ibid.* **1983**, *7*, 201. (c) Shaik, S. S.; Pross, A. *J. Am. Chem. Soc.* **1982**, *104*, 2708. (d) Shaik, S. S. *Ibid.* **1983**, *105*, 4359. (e) Shaik, S. S. *Ibid.* **1984**, *106*, 1227. (f) Pross, A.; Shaik, S. S. *Ibid.* **1981**, *103*, 3702. (g) Pross, A.; Shaik, S. S. *Ibid.* **1982**, *104*, 187. (h) Pross, A.; Shaik, S. S. *Ibid.* **1982**, *104*, 1129. (i) Pross, A.; Shaik, S. S. *Acc. Chem. Res.* **1983**, *16*, 363.
(40) Shaik, S. S. *Progr. Phys. Org. Chem.* **1984**, *15*, 197.

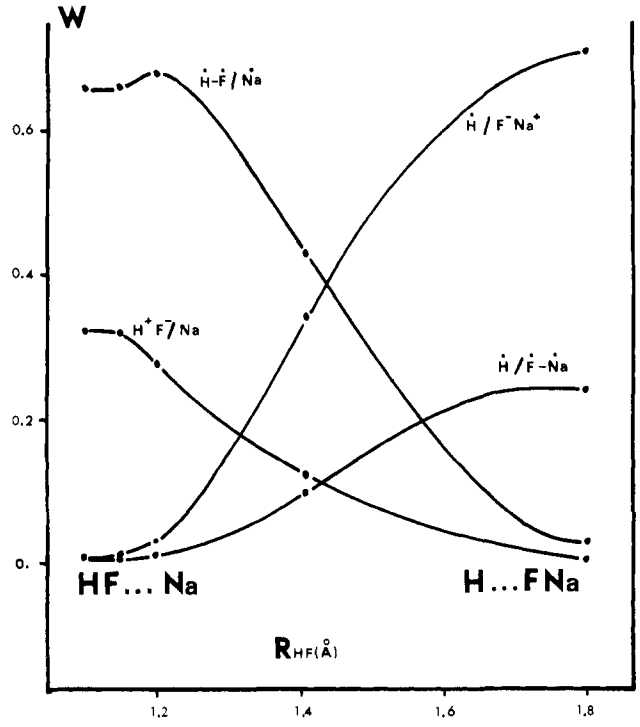

Figure 7. Calculated weights (W) of the optimized structures involved in the thermal reaction 2, as functions of the RC.

behavior of these curves is relatively easy to predict and to connect to thermodynamical constants. Thus, Shaik was able to predict a vast series of activation energies for several families of reactions. The central hypothesis that Shaik postulated is that the VBWFs give a faithful description of the adiabatic ground-state behavior, except in the transition-state region where a gap between VBWF surfaces and adiabatic ones exists, but should remain small. To our knowledge, the diagrams displayed in Figure 6 constitute the first computational confirmation of Shaik's hypothesis. Indeed, in the three reactions the adiabatic curves remain quite close to the quasi-diabatic VB ones, and the avoided crossing stabilization is small, being never larger than 14 kcal/mol. More, the geometries of the transition states, yet determined at the SCF level, correspond almost exactly to the locus of the diabatic curve crossings, as predicted by Shaik. All these results suggest that it is meaningful to think in terms of VBWFs to get an estimate of the reaction profile.

It is interesting to make a connection between the VBWF curves of reaction 2 and the harpooning model. An examination of the VB calculations reveals that the Na–F/H VBWF is mainly ionic in nature, in the vicinity of the transition state; i.e., it is best represented as $Na^+F^-/\dot{H}$, while the Na/F–H VBWF is mainly covalent. It appears on the diagram that the transition state corresponds to a switch from the $\dot{N}a/\dot{F}$–$\dot{H}$ surface to the $Na^+F^-/\dot{H}$ one. This means that the sodium atom transfers an electron to the hydrogen fluoride, and subsequently attracts the HF^- anion and releases the H atom. To have a more quantitative illustration of this phenomenon, we have computed the weights[41] of the ionic and covalent optimized structures and plotted them against the reaction advancement (see Figure 7). The left side of the diagram, corresponding to the HF···Na cluster in which HF is in its equilibrium geometry, displays important $\dot{H}$–$\dot{F}/\dot{N}a$ (covalent) and $H^+F^-/\dot{N}a$ (ionic) structures, in a ratio of approximately 2:1. As the H–F bond is stretched, it becomes slightly more covalent and loses some importance to the benefit of the nascent Na–F bond, which becomes predominant at the right end of the diagram, with an ionic:covalent ratio of about 3:1. The transition state is the locus of a double curve crossing: the $\dot{H}$–$\dot{F}/\dot{N}a$ (covalent) and $\dot{H}/F^-Na^+$ (ionic) curves, on the one hand, the $\dot{H}/\dot{F}$–$\dot{N}a$ (covalent) and $H^+F^-/\dot{N}a$ (ionic), on the other hand, the two latter structures being clearly minor. Therefore, the reaction consists of a passage from a covalent $\dot{H}$–$\dot{F}/\dot{N}a$ structure to an ionic $\dot{H}/F^-Na^+$ one, thus clearly emphasizing the harpooning mechanism.

Conclusion

We have shown that a dialectic use of MO and VB correlation diagrams brings about complementary insights on chemical reactivity. The adiabatic PESs resulting from large CI calculations, involving a large number of reference electronic configurations, are of complex nature, and, very often what is gained in numerical accuracy is lost in chemical information. The use of a VB technique restores most of the chemical significance. It is noteworthy that the various ionic and covalent VB configurations are selected on familiar grounds, and that their optimized structures are determined through small dimension calculations. We thus get quasi-diabatic surfaces whose behavior is easy to follow along a given RC. These surfaces, in turn, yield adiabatic VB PESs, which, in spite of the small number of correlated electrons, give results that are in qualitative agreement with SCF–CI data. A clear understanding of the electronic mechanisms arises from the interplay between ionic and covalent VB surfaces, and the various electronic features of the "harpooning" mechanism thus have been quantitatively specified. The comparison of quasi-diabatic and adiabatic VB surfaces also quantitatively confirms the validity of Shaik's diagrams, thus comforting their predicting power.

Although limited, our exploratory survey yields clear-cut conclusions regarding the feasibility of the various reactions, in the GS. No activation barrier is found along the SCF–CI surface of the exothermic reactions: NaF + H → Na + FH, NaH + F → Na + HF (respectively the reverse of reactions 2), and F + NaH → FNa + H (reaction 4). A very small one is found along the latter reaction in the VB calculation.

In the excited states, attention has been focused on the excited sodium atom reactivity. The only exothermic channel is found in reaction 2. The formation of stable exciplexes is predicted in a geometry close to that of the GS SCF transition state. The corresponding potential energy wells are deeper for the Rydberg states of high quantum number than for the low-lying 3P states. Important fluorescence red shifts are predicted for all these states. The quasi-contact situation with the GS surface found in the 3P exciplexes provides a potentially reactive channel, driving the reaction from the latter states to the GS of Na + FH. No adiabatic channel exists for the states of higher energy, but we have shown that diabatic coupling with the dissociative charge-transfer surface ($Na^+\cdots FH^-$) provides a potentially reactive channel, whose efficiency might be important. Since all these possibilities have not yet been experimentally tested, we hope that further experimental work will be made in this field.

Acknowledgment. The calculations have been performed at the Centre Inter-Régional de Calcul Electronique (CIRCE) in Orsay. We gratefully acknowledge the CIRCE for generous contribution of computer time.

Registry No. Na, 7440-23-5; HF, 7664-39-3; H_2, 1333-74-0.

(41) We have used Chirgwin and Coulson's well-known definition[42] of the weight W_n of a VB structure as a function of its coefficient C_n: $W_n = C_n^2 + \sum_{m \neq n} C_m C_n S_{mn}$, where S_{mn} is the overlap between the two VB structures m and n.

(42) Chirgwin, B. H.; Coulson, C. A. *Proc. R. Soc. London, Ser. A* **1950**, *201*, 196.